Computational Mechanics (1993) 11, 341–354

Computational Mechanics

The simultaneous use of 4 × 4 and 2 × 2 bilinear stress elements for viscoelastic flows

Georgios C. Georgiou[1] and **Marcel J. Crochet**

Unité de Mécanique Appliquée, Université Catholique de Louvain, 2 Place du Levant, B-1348 Louvain-la-Neuve, Belgium

Abstract. Mixed finite elements for viscoelastic flows based on a 4 × 4 sub-linear interpolation for the extra stress components satisfy the Babuska–Brezzi condition and are highly stable. They have been proved to be quite satisfactory in solving problems with strong stress boundary layers. In this work, we examine the simultaneous use of 4 × 4 and 2 × 2 bilinear stress elements in an attempt to reduce the computational cost without sacrificing the accuracy. The 4 × 4 bilinear elements are employed in regions where the stress field is anticipated to be steep while the 2 × 2 elements carry the burden elsewhere with a much smaller number of stress nodes. Additional constraints along the sides shared by different elements are necessary in order to preserve conformity. The method is applied to the creeping flow of a Maxwell fluid around a sphere falling along the axis of a cylindrical tube. Results are given for three mixed finite element formulations: the Galerkin method, the consistent streamline-upwind/Petrov–Galerkin method (SUPG) and the non-consistent streamline-upwind method (SU). Particular emphasis is given on the calculated drag correction factors. The effect of the sphere/cylinder diameter ratio is also examined.

1 Introduction

In 1987, Marchal and Crochet (1987) introduced a mixed finite element for calculating viscoelastic flow. It is characterized by a finite element representation of the stresses in terms of 4 × 4 bilinear sub-elements. Unlike the biquadratic or other elements previously proposed in the literature, their element satisfies the Babuška–Brezzi condition for convergence (Babuška 1973; Brezzi 1974; Fortin and Pierre 1989) at least at the Stokes flow limit, while it leads to stable numerical schemes. It is, however, characterized by a high number of stress nodes per element resulting in a higher computational cost.

Marchal and Crochet (1987) considered successive stress representations using 2 × 2, 3 × 3 and 4 × 4 sub-elements. It was clear that 4 × 4 sub-elements are needed in regions characterized by stress boundary layers or singularities. One may question the effectiveness of covering the entire flow domain with the expensive 4 × 4 sub-elements while they appear to be unnecessary in sub-domains of substantial size. The objective of the present work is to introduce the simultaneous use of 4 × 4 and 2 × 2 bilinear stress elements for the solution of viscoelastic flow problems in order to reduce the total number of unknowns, and consequently the computational cost, without sacrificing the accuracy. The 4 × 4 bilinear elements are used only in those regions where stress boundary layers or singularities are present and the 2 × 2 ones are employed elsewhere.

As in Marchal and Crochet (1987), we consider three mixed finite element formulations:

1. The Galerkin method
2. The consistent streamline-upwind/Petrov–Galerkin method (SUPG)
3. The non-consistent streamline-upwind method (SU)

The Galerkin method converges only at relatively low values of the *We* due to the hyperbolic character of the constitutive equation (Marchal and Crochet 1987). Galerkin/finite element methods are formally accurate but unstable, failing in flows possessing sharp solution gradients or singularities. In order to stabilize the numerical scheme, Marchal and Crochet (1987) introduced the use

[1] Present address: Department of Mathematics, The University of Cyprus, Kallipoleos 75, P.O. Box 537, Nicosia, Cyprus

of the SU and SUPG methods developed by Brooks and Hughes (1982) for the finite element integration of hyperbolic equations.

The SUPG method is accurate and stable for problems in smooth geometries such as the viscoelastic flow in a corrugated tube (Crochet et al. 1990) and around a sphere (Crochet and Legat 1992). The SUPG method is formally more accurate than the Galerkin method (Keunings 1989), but if the solution gradient is not aligned with the streamlines or in the presence of singularities, the method produces oscillatory stress and velocity fields as, for example, in the stick-slip flow of a Maxwell fluid (Marchal and Crochet 1987).

The SU formulation was proposed in Marchal and Crochet (1987) as an alternative to the SUPG method for flow problems with stress singularities. The modified test function is used only for the integration of the purely advective term of the constitutive equation and thus the original problem is modified by the addition of an extra diffusion term. As shown in Crochet et al. (1990); Crochet and Legat (1992) this numerical diffusion vanishes as the mesh is refined but the method converges slowly. The velocity field converges faster than the stress field (Crochet and Legat 1992). The results are accurate at the asymptotic limit where the mesh size goes to zero. The method yields smooth results and is remarkably stable at very high Weissenberg numbers.

The above comments are needed as a background for the study of the numerical schemes described in Sect. 3, where we demonstrate once more the higher accuracy of the SUPG method and the stabilizing character of the SU method. As a test problem for the simultaneous use of 2×2 and 4×4 stress sub-elements, we have chosen the steady flow of a Maxwell fluid around a rigid sphere moving with a constant translational velocity along the axis of a cylindrical tube. Characteristic of this flow is the development of strong boundary layers around the sphere surface whose strength increases with fluid elasticity. These stress boundary layers require local mesh refinement making the problem suitable for our purposes.

It should be pointed out that the sphere problem has been investigated as a benchmark problem by means of several numerical methods: mixed finite elements (Crochet and Legat 1992), boundary elements (Zheng et al. 1990; 1991), finite differences (Chilcott and Rallison 1988), spectral methods (Gervang et al. 1992), and the explicitly elliptic momentum equation (EEME) method (Lunsmann et al. 1992). Recent reviews of numerical simulations in viscoelastic flow may be found in (Crochet 1989; Keunings 1989).

In Sect. 2, we pose the sphere problem and give a literature review of viscoelastic flow in such geometries. The finite element results are discussed in Sects. 4 and 5, and, finally, the conclusions are summarized in Sect. 6.

2 The sphere problem

We consider the flow of a viscoelastic fluid around a rigid sphere of radius R falling with a (terminal) velocity U along the symmetry axis of a tube of radius R_C. In our calculations, it is actually assumed that the sphere is motionless and the wall moves with velocity U instead. The flow is axisymmetric and we employ cylindrical coordinates (r, z) as shown in Fig. 1. For steady, isothermal and incompressible flow, the momentum and continuity equations are as follows:

$$-\nabla p + \nabla \cdot \mathbf{T} + \mathbf{f} = \rho \mathbf{v} \cdot \nabla \mathbf{v}, \quad \nabla \cdot \mathbf{v} = 0, \tag{1,2}$$

where p is an arbitrary isotropic pressure, $\mathbf{T}$ is the extra-stress tensor, $\mathbf{f}$ denotes the body force, ρ is the density, and $\mathbf{v}$ is the velocity vector.

In this work, we will be concerned with the upper-convected Maxwell fluid, the constitutive

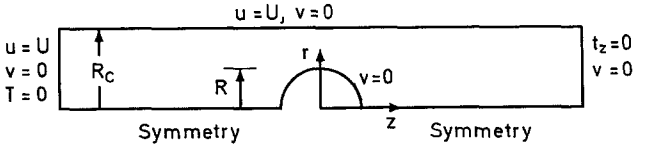

Fig. 1. Geometry and boundary conditions

equation of which is as follows:

$$\mathbf{T} + \lambda \overset{\nabla}{\mathbf{T}} - 2\eta \mathbf{d} = \mathbf{0}, \tag{3}$$

where λ is the relaxation time, η is the (constant) shear viscosity, $\overset{\nabla}{\mathbf{T}}$ is the upper-convected derivative of the stress tensor, defined as:

$$\overset{\nabla}{\mathbf{T}} = \mathbf{v}\cdot\nabla\mathbf{T} - (\nabla\mathbf{v})^T\cdot\mathbf{T} - \mathbf{T}\cdot\nabla\mathbf{v}, \tag{4}$$

$\mathbf{d}$ is the rate-of-deformation tensor defined by

$$\mathbf{d} = \tfrac{1}{2}[(\nabla\mathbf{v}) + (\nabla\mathbf{v})^T]. \tag{5}$$

$\nabla\mathbf{v}$ is the velocity-gradient tensor, and, finally, the superscript T denotes the transpose.

The boundary conditions are shown in Fig. 1. Essential boundary conditions for $\mathbf{v}$ and $\mathbf{T}$ are taken at the inlet. The radial velocity and the normal force are vanishing at the outlet plane. The velocity is set equal to zero along the sphere surface and equal to U along the wall.

We nondimensionalize the governing equations by scaling the velocity components by U, the lengths by R and the pressure and stress components by $\eta U/R$. With the body force neglected, this scaling yields two dimensionless numbers, the Reynolds number, Re, and the Weissenberg number, We:

$$Re \equiv \frac{\rho U R}{\eta}; \quad We \equiv \frac{\lambda U}{R}. \tag{6}$$

The drag exerted on the sphere constitutes a very interesting quantity to calculate and it is commonly used to compare the various numerical techniques (Crochet and Legat 1992; Zheng et al. 1990) and/or experimental measurements (Chmielewski et al. 1990; Tirtaatmadja et al. 1990). For creeping flow in an unbounded Newtonian fluid, the drag force F_∞^N is given by Stoke's law:

$$F_\infty^N = 6\pi\eta R U. \tag{7}$$

In the present paper, we consider creeping flow in tubes of finite diameter and we are thus interested in the wall effect. For Newtonian fluids, the wall effect is accounted by the *Faxen correction factor* K_w (Chmielewski et al. 1990), defined as the ratio of the drag in a bounded medium to that in an unbounded medium:

$$K_w = \frac{F^N}{F_\infty^N} = \frac{1}{1 - \left(\frac{R}{R_C}\right) W\left(\frac{R}{R_C}\right)}, \tag{8}$$

where the polynomial expansion W is given by:

$$W\left(\frac{R}{R_C}\right) = 2.1044 - 2.088\left(\frac{R}{R_C}\right)^2 + 0.9481\left(\frac{R}{R_C}\right)^4 + 1.372\left(\frac{R}{R_C}\right)^5 - 3.87\left(\frac{R}{R_C}\right)^7 + 4.19\left(\frac{R}{R_C}\right)^9. \tag{9}$$

With only a few exceptions (e.g., Chhabra and Uhlherr 1988), for sphere motion in viscoelastic fluids, the wall effect on the drag coefficient is significant albeit less pronounced than for Newtonian fluids. Tirtaatmadja et al. (1990) using fluid M1 and Chmielewski et al. (1990) using a Boger fluid found that the wall effect is similar to that for the Newtonian fluids, at least for R/R_C up to 0.15 (hence, the Faxen correction can be used), whereas Mena et al. (1987) found that wall effects are much less appreciable for their non-Newtonian solutions than for the Newtonian case for similar value of R/R_C and that wall corrections are relatively unimportant in determining the drag force for R/R_C less than 1/15. Hassager and Bisgaard (1983) have also observed relatively significant wall effects in experiments with a solution of polyacrylamide in glycerine.

The effect of fluid elasticity on the drag coefficient is not fully understood. A useful quantity accounting for the deviation from Stokes's law is the *drag correction factor* K, defined as the ratio of the drag exerted on the sphere, F^V, to that exerted by an unbounded Newtonian fluid:

$$K = \frac{F^V}{F^N_\infty} = \frac{F^V}{6\pi\eta UR}. \tag{10}$$

When a wide cylinder is used, the fluid elasticity has little effect on the drag correction factor for low values of the Weissenberg number, as indicated by small perturbation solutions for Oldroyd-type fluids (Leslie 1961; Giesekus 1963) and a third-order Rivlin–Ericksen fluid (Caswell and Schwarz 1962; Mena and Caswell 1974). Perturbation solutions are obtained as a convergent series in powers of the Weissenberg number:

$$C_D = C^N_D[1 - O(We)^2 + O(We)^4 + \cdots]. \tag{11}$$

Note that Eq. (11) is valid only for slightly viscoelastic flow in the creeping limit. Its predictions are substantiated by a plethora of experimental results (Chmielewski et al. 1990; Mena et al. 1987; Broadbent and Mena 1974; Chhabra et al. 1980) and by numerical simulations with the Maxwell model (Hassager and Bisgaard 1983), with an Oldroyd-type model (Tiefenbruck and Leal 1982) and with the Phan-Thien-Tanner model (Carew and Townsend 1988). From experimental and numerical evidence, it appears that the quadratic drag departure of Eq. (11) holds for values of We much higher than what one would expect from an asymptotic analysis (Mena et al. 1987).

When a narrow cylinder is used, fluid elasticity appears to reduce K (with the exception of few experimental and numerical results to be discussed below). The experiments of Chhabra et al. (1990); Mena et al. (1987), and Chmielewski et al. (1990) with corn-syrup-based Boger fluids and of Hassager and Bisgaard (1983) with an 1% solution of polyacrylamide in glycerine showed that, as We increases, K decreases monotonically reaching eventually a plateau. Mena et al. (1987) found that for their Boger fluid the drag reduction was initially quadratic as predicted by Eq. (11), but that was not true for their viscoelastic Separan solution due to the fact that shear-thinning effects dominated enhancing the drag reduction. Drag reduction has also been predicted in numerical calculations: by Chilcott and Rallison (1988) using an FENE-dumbbell model with a set of parameters representing a constant-viscosity elastic fluid; by Hassager and Bisgaard (1983) and Crochet and Legat (1992) using the Maxwell model; by Tiefenbruck and Leal (1982) and Zheng et al (1990) using the Oldroyd model; and by Sugeng and Tanner (1986) and Carew and Townsend (1988) using the Phan-Thien-Tanner model (Carew and Townsend 1988).

In a few cases, however, drag enhancement with fluid elasticity has been detected. Acharya et al. (1976) found negligible influence of viscoelasticity on the drag coefficient using polyethylene and polyacrylamide solutions. Chmielewski et al. (1990) using a polyisobutylene/polybutene-based Boger fluid found that K remains constant at low We and then increases monotonically. Tirtaatmadja et al. (1990) in experiments with fluid M1 found that K decreases slightly reaching a minimum at a moderate value of We and it then increases monotonically surpassing the Stokes value. Chilcott and Rallison (1988) have been able to simulate this behavior using an FENE model with appropriate parameters. Tirtaatmadja et al. (1990) suggest that these different behaviors of K are due to different polymer-solvent configurations. Other researchers attribute the increase in the drag coefficient to the different flow patterns in the downstream wake where the velocity decays much more slowly than that of a Newtonian liquid due to the presence of a thin region of highly extended polymer (Chilcott and Rallison 1988; Harlen 1990).

In the present review, we have not considered the effect of inertia. Even for creeping flow, it is clear that both shear thinning and viscoelasticity play important roles, while accurate numerical solutions are hard to obtain in view of the presence of the stress boundary layers. Our purpose below is to investigate how the use of accurate elements within the stress boundary layers would let us perform calculations at an affordable cost. Although we limit ourselves to the flow of a Maxwell fluid, the method is entirely applicable to other types of constitutive equations.

3 Finite element methods

The finite element method is used to calculate the unknown fields, $\mathbf{v}, p$ and $\mathbf{T}$. The flow domain Ω is discretized by means of quadrilateral elements. To interpolate $\mathbf{v}$ and p we use biquadratic, Φ^j ($P^2 - C^0$), and bilinear, Ψ^j ($P^1 - C^0$), trial functions respectively:

$$\mathbf{v} = \sum_j^{N_v} \mathbf{v}^j \Phi^j, \quad p = \sum_j^{N_p} p^j \Psi^j, \tag{12,13}$$

where $\mathbf{v}^j, p^j$ are the unknown nodal values of $\mathbf{v}$ and p, and N_v, N_p are the numbers of velocity and pressure nodes. For the stresses, we use the 4 × 4 bilinear sub-elements developed by Marchal and Crochet (1987) in regions where sharp stress gradients are anticipated (e.g., near the surface of the sphere), and the 2 × 2 elements in the rest of the computational domain. We will show below why we have not used in these regions the biquadratic mixed element MIX1 discussed by Crochet et al. (1984). Letting χ^j represent the stress trial functions, $\mathbf{T}^j$ denote the unknown nodal values of the stress tensor, and N_T be the number of stress nodes, we have:

$$\mathbf{T} = \sum_j^{N_T} T^j \chi^j. \tag{14}$$

As mentioned in the introduction, we consider three mixed finite element formulations: the Galerkin, the SUPG and the SU methods. What is different in the above formulations is the discretization of the constitutive equation. In all cases, the continuity equation is weighted by Ψ^i and the momentum equation by Φ^i:

$$\int_\Omega \nabla\cdot\mathbf{v}\,\Psi^i d\Omega = 0, \quad i = 1, 2, \ldots, N_p, \tag{15}$$

$$\int_{\partial\Omega} \mathbf{n}\cdot(-p\mathbf{I} + \mathbf{T})\Phi^i ds - \int_\Omega [(-p\mathbf{I} + \mathbf{T})\cdot\nabla\Phi^i + \rho\mathbf{v}\cdot\nabla\mathbf{v}\Phi^i] d\Omega = 0, \quad i = 1, 2, \ldots, N_v, \tag{16}$$

where $\mathbf{n}$ is the outward unit normal vector to the boundary $\partial\Omega$.

In the Galerkin method, the constitutive equation is weighted by χ^i (the test functions are identical to the trial or weight functions):

$$\int_\Omega (\mathbf{T} + \lambda\overset{\nabla}{\mathbf{T}} - 2\eta\mathbf{d})\chi^i d\Omega = 0, \quad i = 1, 2, \ldots, N_T. \tag{17}$$

In the SUPG method, a modified test function $\hat{\chi}^i$ is employed:

$$\hat{\chi}^i = \chi^i + k\mathbf{v}\cdot\nabla\chi^i. \tag{18}$$

The function k is given by:

$$k = \frac{\alpha}{2}\frac{(u_\xi^2 + u_\eta^2)^{1/2}}{\mathbf{v}\cdot\mathbf{v}}, \tag{19}$$

where α is the streamline upwinding coefficient, and u_ξ, u_η are defined as:

$$u_\xi = \mathbf{v}_0\cdot\mathbf{h}_\xi, \quad u_\eta = \mathbf{v}_0\cdot\mathbf{h}_\eta.$$

In the case of the 4 × 4 stress elements, $\mathbf{v}_0$ is the velocity at the centroid of a sub-element and the vectors $\mathbf{h}_\xi, \mathbf{h}_\eta$ have a length of the same order as the sub-element size (see Marchal and Crochet 1987). Shown in Fig. 2 are the two alternative definitions, $D1$ and $D2$, we have used in the case of the 2 × 2 stress elements for vectors $\mathbf{v}_0, \mathbf{h}_\xi$ and $\mathbf{h}_\eta$. In $D1$ these vectors are defined over the sub-elements, and in $D2$ they are defined over the quadrilaterals resulting from the 4 × 4 partition of the element in a fashion similar to that of the 4 × 4 stress elements.

In the SU method, the modified test function is used only for the integration of the purely advective term $\mathbf{v}\cdot\nabla\mathbf{T}$ of the constitutive equation:

$$\int_\Omega (\mathbf{T} + \lambda\overset{\nabla}{\mathbf{T}} - 2\eta\mathbf{d})\chi^i d\Omega + \int_\Omega \lambda\mathbf{v}\cdot\nabla\mathbf{T}k\mathbf{v}\cdot\nabla\chi^i d\Omega = 0, \quad i = 1, 2, \ldots, N_T. \tag{20}$$

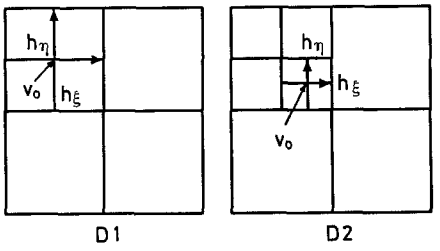

2

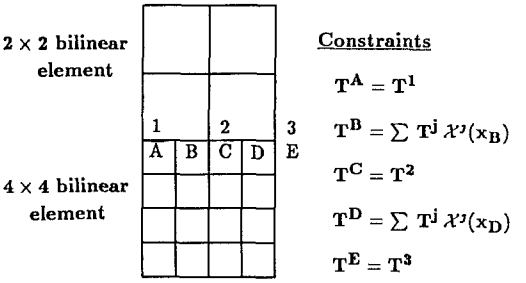

3

Figs 2 and 3. 2 Alternative definitions of $\mathbf{v}_0$, $\mathbf{h}_\xi$ and $\mathbf{h}_\eta$ for the 2 × 2 stress element. 3 Constraints along a side shared by 2 × 2 and 4 × 4 stress elements

In order to preserve the conformity of the elements, additional constraints along the sides shared by 4 × 4 and 2 × 2 elements are required. Let us use the indices 1–3 for the 2 × 2 stress nodes and A–E for the 4 × 4 ones along such a side, as illustrated in Fig. 3. We demand that the stresses at the bilinear nodes A–E are the same for both elements. Nodes A, C and E coincide with nodes 1, 2 and 3, respectively, and so do the corresponding nodal stress values. At nodes B and D we have:

$$\mathbf{T}^B = \sum_{j=1}^{3} \mathbf{T}^j \chi^j_{2\times 2}|_B = (\mathbf{T}^1 + \mathbf{T}^2)/2 = (\mathbf{T}^A + \mathbf{T}^C)/2 \tag{21}$$

$$\mathbf{T}^D = \sum_{j=1}^{3} \mathbf{T}^j \chi^j_{2\times 2}|_D = (\mathbf{T}^2 + \mathbf{T}^3)/2 = (\mathbf{T}^C + \mathbf{T}^E)/2 \tag{22}$$

where $\chi^j_{2\times 2}$ are the shape functions over the 2 × 2 element. Similar constraints have been used by Marchal et al. (1984) when they adaptively refined a biquadratic mesh introducing two biquadratic elements under side 1–2. As in Marchal et al. (1984), instead of replacing the discretized stress equations at nodes B and D by the constraints (21) and (22), we eliminate the unknowns at these nodes by modifying the shape functions over the 4 × 4 element. Over the sub-elements adjacent to the 2 × 2 element we have:

$$\mathbf{T} = \mathbf{T}^A \chi^A_{4\times 4} + \mathbf{T}^B \chi^B_{4\times 4} + \mathbf{T}^C \chi^C_{4\times 4} + \mathbf{T}^D \chi^D_{4\times 4} + \mathbf{T}^E \chi^E_{4\times 4}. \tag{23}$$

By virtue of constraints (21) and (22), Eq. (23) becomes:

$$\mathbf{T} = \mathbf{T}^A(\chi^A_{4\times 4} + \tfrac{1}{2}\chi^B_{4\times 4}) + \mathbf{T}^C(\chi^C_{4\times 4} + \tfrac{1}{2}\chi^B_{4\times 4} + \tfrac{1}{2}\chi^D_{4\times 4}) + \mathbf{T}^E(\chi^E_{4\times 4} + \tfrac{1}{2}\chi^D_{4\times 4}), \tag{24}$$

and therefore the modified shape functions over the 4 × 4 element read as follows:

$$\chi^A_{\mathrm{NEW}} = \chi^A_{4\times 4} + \tfrac{1}{2}\chi^B_{4\times 4}, \quad \chi^C_{\mathrm{NEW}} = \chi^C_{4\times 4} + \tfrac{1}{2}\chi^B_{4\times 4} + \tfrac{1}{2}\chi^D_{4\times 4}, \quad \chi^E_{\mathrm{NEW}} = \chi^E_{4\times 4} + \tfrac{1}{2}\chi^D_{4\times 4}.$$

It is now clear why we have combined 4 × 4 and 2 × 2 mixed elements instead of 4 × 4 and biquadratic (MIX1) elements. At the interface between 4 × 4 and biquadratic elements, we could not possibly obtain (in general) a C^0 continuity of the extra stress field while the constitutive equations contain stress derivatives. With the constraints (21) and (22), we obtain a linear interpolation of the stress fields between nodes A, C and E on both sides of the interface. Another reason is that the SU and SUPG methods have been essentially developed for bilinear shape functions.

The discretized continuity, momentum and constitutive equations are solved simultaneously by means of the Newton–Raphson method. The calculation of the drag exerted on the sphere amounts to the summation of the nodal forces in the z-direction along the sphere surface $\partial\Omega_S$:

$$F^V = \sum_{i \text{ on } \partial\Omega_S} \mathbf{e}_z \cdot \int_{\Omega} [(-p\mathbf{I} + \mathbf{T})\cdot\nabla\Phi^i + \rho\mathbf{v}\cdot\nabla\mathbf{v}\Phi^i]\, d\Omega, \tag{25}$$

where $\mathbf{e}_z$ is the unit vector in the z-direction.

4 Numerical results: $(R_C/R) = 2$

In order to demonstrate the advantage of using both types of elements for solving viscoelastic flow problems endowed with stress boundary layers, we first examine the well-documented case of $(R_C/R) = 2$ and employ the meshes I and II used in Crochet and Legat (1992) (see Fig. 4). Results for other values of (R_C/R) will be given in the next section.

The entry and exit lengths are equal to $15R$ and $30R$ respectively. We observe that the central portion of the meshes shown in Fig. 4 is made of a series of layers of quadrilateral elements. It is thus convenient to fill the first N_l layers with 4 × 4 elements and the rest with 2 × 2 ones. The main characteristics of the meshes are given in Table 1 for different numbers of 4 × 4-element layers.

In the sequence, we first discuss the results with full 4 × 4-element and full 2 × 2-element meshes, and then we proceed to the results obtained when the two elements are used simultaneously. Note that in all the calculations of this work, inertia is neglected ($Re = 0$) and an increment of 0.1 is used to proceed to a higher We. We do not pursue the calculations with a different increment for We when the method diverges.

4.1 Results with the 4 × 4 stress elements

We have first examined the results obtained with 4 × 4 stress elements using the Galerkin, the SUPG and the SU methods. The SUPG and SU results are the same as those of Crochet and Legat (1992). Table 2 gives the calculated values of K for all the methods. Notice that a streamline upwinding coefficient $\alpha = 0.5$ was used in Crochet and Legat (1992). It is generally conceded that what is important is the form of the streamline upwinding function and not the value of α (Brooks and Hughes 1982). Nevertheless, we would like to point out that this is true only when the mesh is adequately refined. The effect of the streamline upwinding coefficient on K is illustrated in Fig. 5 where we also show the values of Crochet and Legat (1992) obtained with the SUPG method and mesh III. For We up to 0.4, K is practically independent of α. As α increases the method converges at higher values of the We but the numerical diffusion introduces a serious error and a minimum is observed before divergence occurs. As the mesh is refined, the error decays and the minimum moves towards the converged solution and eventually disappears (Crochet and Legat 1992; Lunsmann et al. 1992). Unless otherwise indicated, the value $\alpha = 0.5$ is employed hereafter.

Table 2 summarizes the well-known behavior of the various numerical techniques for smooth viscoelastic problems. A finer mesh allows one to reach higher values of the Weissenberg number. The SUPG method converges at slightly higher values than the Galerkin method. The SU method is stable and allows one to reach high values of We but it converges slowly with mesh refinement. The SU results are best used in conjunction with a Richardson type of extrapolation (Crochet et al. 1990; Crochet and Legat 1992).

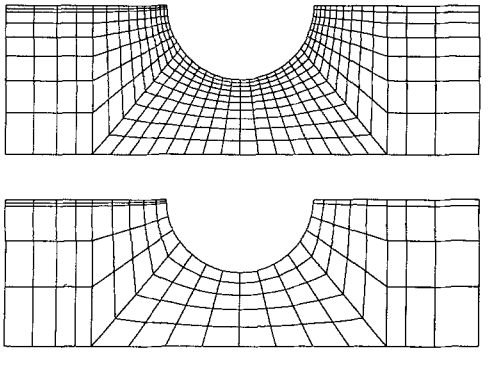

Fig. 4. Central portions of the finite element meshes

Table 1. Mesh characteristics

N_l	Number of 4 × 4 elements	Degrees of freedom
Mesh I: 207 elements; 925 velocity nodes		
0	0	5806
1	17	6766
2	34	7590
3	51	8414
4	68	9238
Full 4 × 4	207	16126
Mesh II: 510 elements; 2175 velocity nodes		
0	0	13628
1	31	15372
4	124	19860
7	217	24348
9	279	27340
Full 4 × 4	510	38644

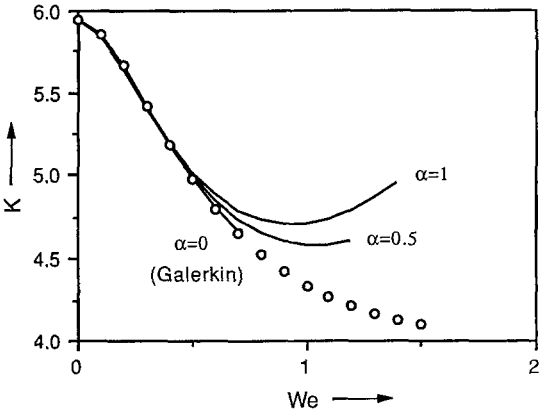

Fig. 5. Effect of the streamline-upwinding coefficient α on the drag correction factor K; SU method, mesh I, full 4 × 4; ○: values of Crochet and Legat (1992) with the SUPG method and mesh III

Table 2. Calculated values of K with 4 × 4 stress elements; mesh I

We	Galerkin		SUPG		SU	
	Mesh I	Mesh II	Mesh I	Mesh II	Mesh I	Mesh II
0.0	5.9490	5.9476	5.9490	5.9476	5.9490	5.9476
0.1	5.8639	5.8622	5.8638	5.8620	5.8527	5.8565
0.2	5.6625	5.6598	5.6624	5.6598	5.6484	5.6523
0.3	5.4236	5.4198	5.4235	5.4197	5.4145	5.4144
0.4	5.1923	5.1873	5.1920	5.1872	5.1947	5.1873
0.5	4.9871	4.9803	4.9867	4.9801	5.0066	4.9884
0.6	4.8130	4.8034	4.8125	4.8031	4.8546	4.8219
0.7	4.6699	4.6553	4.6697	4.6548	4.7381	4.6864
0.8	Diverges	4.5332	4.5593	4.5320	4.6548	4.5785
0.9		4.4346	Diverges	4.4314	4.6025	4.4946
1.0		Diverges		4.3502	4.5788	4.4312
1.1				4.2862	4.5815	4.3854
1.2				Diverges	4.6077	4.3546
1.3					Diverges	4.3368
1.4						4.3302
1.5						4.3335
1.6						4.3454
1.7						4.3650
1.8						4.3915
1.9						Diverges

4.2 *Results with the 2 × 2 stress elements*

As mentioned in the previous section, we examined two definitions, $D1$ and $D2$, of the vectors $\mathbf{v}_0$, $\mathbf{h}_\xi$ and $\mathbf{h}_\eta$ as shown in Fig. 2. The two definitions yield equivalent streamline upwinding functions at the limit of an infinitely refined mesh. With the meshes employed here, however, definition $D2$ appears to be superior. The SUPG method diverges even at low We when definition $D1$ is used. The SU method gives much better estimates for the drag correction when $D2$ is used, as shown in Fig.6. Furthermore, definition $D2$ gives more stable results than $D1$ and it is consistent with the definition used with the 4 × 4 stress elements. The results obtained with definition $D1$ and the SU method are tainted upstream and downstream by wiggles of a wavelength equal to the element size which grow as the We increases. (Oscillations are unavoidable with the 2 × 2 as well as with the biquadratic stress elements but they appear at relatively higher values of We when the Galerkin method or the other methods with definition $D2$ are used.) All the following calculations involving 2 × 2 stress elements have been performed using definition $D2$.

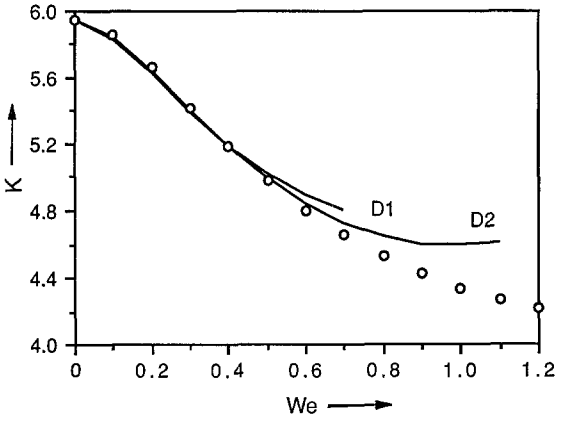

Fig. 6. Calculated values of K with the 2 × 2 stress elements and mesh I; $D1$: definition of vectors $\mathbf{v}_0$, $\mathbf{h}_\xi$ and $\mathbf{h}_\eta$ over the sub-elements; $D2$: definition of the vectors over the quadrilaterals resulting from the 4 × 4 partition of the element; ○: values of Crochet and Legat (1992) with the SUPG method and mesh III

Table 3. Calculated values of K with 2 × 2 stress elements. The values in parentheses correspond to unacceptable finite-element solution ($u_{\min} < -\varepsilon$)

We	Galerkin		SUPG		SU	
	Mesh I	Mesh II	Mesh I	Mesh II	Mesh I	Mesh II
0.0	5.9461	5.9473	5.9463	5.9473	5.9461	5.9473
0.1	5.8606	5.8619	5.8604	5.8618	5.8487	5.8560
0.2	5.6571	5.6595	5.6562	5.6593	5.6419	5.6517
0.3	5.4146	5.4193	5.4129	5.4190	5.4045	5.4138
0.4	5.1788	5.1865	5.1763	5.1862	5.1809	5.1866
0.5	4.9695	(4.9808)	4.9660	4.9788	4.9894	4.9878
0.6	Diverges	Diverges	4.7883	(4.8013)	4.8354	4.8216
0.7			Diverges	Diverges	4.7196	4.6864
0.8					4.6412	4.5789
0.9					4.5984	(4.4953)
1.0					4.5874	(4.4323)
1.1					4.6026	(4.3869)
1.2					Diverges	(4.3568)
1.3						(4.3401)
1.4						(4.3354)
1.5						(4.3418)
1.6						(4.3588)
1.7						(4.3872)
1.8						(4.4285)
1.9						(4.4813)
2.0						(4.5421)
2.1						Diverges

Another issue is the numerical integration of the constitutive equation. A 3 × 3 Gauss–Legendre quadrature is exact with the Galerkin method, and adequate with the SU method when applied over the quadrilaterals resulting from the 4 × 4 partition of the elements. A difficulty arises with the SUPG method. A Gauss–Legendre quadrature appears to be inappropriate because of the presence of the non-polynomial term:

$$\frac{\alpha}{2}\frac{(u_\xi^2+u_\eta^2)^{1/2}}{\mathbf{v}\cdot\mathbf{v}}\mathbf{T}\cdot\mathbf{v}\cdot\nabla\chi^i.$$

The above term becomes singular in regions where the velocity goes to zero (i.e., at the surface of the sphere). Notice that the same singularity occurs with the 4 × 4 elements as well, and becomes weaker as the mesh is refined. It vanishes at the limit of an infinitely refined mesh, because the velocity term in the denominator is cancelled by the velocity $\mathbf{v}_0$ used to define u_ξ and u_η. It is worthwhile to mention that the singularity effect is more severe with definition $D1$ for the vectors $\mathbf{v}_0, \mathbf{h}_\xi$ and $\mathbf{h}_\eta$ than with definition $D2$ and this provides an explanation for the divergence of the SUPG method with $D1$. We decided to use a 3 × 3 integration over the quadrilaterals expecting to improve the accuracy by refining the mesh rather than by increasing the order of integration or by changing the integration rule.

The calculated values of the stress correction factor are listed in Table 3. They confirm earlier results obtained with biquadratic stress elements used before the development of the 4 × 4 element. The Galerkin and the SUPG methods fail at low values of *We* while the situation does not improve with mesh refinement. The SU method converges at much higher values of *We* than the Galerkin and the SUPG methods and its range of convergence increases considerably with mesh refinement. Nevertheless, the finite element solution becomes oscillatory and eventually unacceptable above a critical value of the *We*, signaling the loss of convergence and the need for further mesh refinement (most necessary in the neighborhood of the sphere). As with the biquadratic stress elements (Marchal et al. 1984), the oscillations originate in the small element at the rear stagnation point, where the tensor $\left(\mathbf{T}+\frac{\eta}{\lambda}\mathbf{I}\right)$ loses its positive definiteness and one detects negative values for the axial velocity component. We consider the finite element solution acceptable if the minimum value of u is not greater in magnitude than the tolerance $\varepsilon = 10^{-4}$ used in our calculations.

4.3 Simultaneous use of 4 × 4 and 2 × 2 bilinear stress elements

In the preceding subsections, we have seen that the low-cost 2 × 2 stress elements are unstable allowing oscillations to develop around the sphere surface. On the other hand, the highly stable

Table 4. Calculated values of K with the Galerkin method; mesh I

We	Full 4 × 4	$N_t = 1$	$N_t = 0$
0.0	5.9490	5.9464	5.9461
0.1	5.8639	5.8615	5.8606
0.2	5.6625	5.6599	5.6571
0.3	5.4236	5.4203	5.4146
0.4	5.1923	5.1881	5.1788
0.5	4.9871	4.9822	4.9695
0.6	4.8130	4.8084	Diverges
0.7	4.6699	Diverges	
0.8	Diverges		

Table 5. Calculated values of K with the SUPG method; mesh I

We	Full 4 × 4	$N_t = 1$	$N_t = 0$
0.0	5.9490	5.9465	5.9463
0.1	5.8638	5.8612	5.8604
0.2	5.6624	5.6589	5.6562
0.3	5.4235	5.4187	5.4129
0.4	5.1920	5.1863	5.1763
0.5	4.9867	4.9807	4.9660
0.6	4.8125	4.8070	4.7883
0.7	4.6697	4.6646	Diverges
0.8	4.5593	Diverges	
0.9	Diverges		
1.0			

Table 6. Calculated values of K with the SU method; mesh I

We	Full 4 × 4	$N_t = 1$	$N_t = 0$
0.0	5.9490	5.9464	5.9461
0.1	5.8527	5.8495	5.8487
0.2	5.6484	5.6443	5.6419
0.3	5.4145	5.4094	5.4045
0.4	5.1947	5.1888	5.1809
0.5	5.0066	5.0003	4.9894
0.6	4.8546	4.8486	4.8354
0.7	4.7381	4.7331	4.7196
0.8	4.6548	4.6515	4.6412
0.9	4.6025	4.6015	4.5984
1.0	4.5788	Diverges	4.5874
1.1	4.5815		4.6026
1.2	4.6077		Diverges
1.3	Diverges		

4 × 4 stress elements are costly. We now proceed to the simultaneous use of these elements in an attempt to obtain accurate results with a lower computational cost. Let us first examine the effect of using both types of elements on the coarse mesh I, shown in Fig. 4. We limit ourselves to $N_l = 1$, i.e., only the first layer of quadrilateral elements near the sphere is made of 4 × 4 elements. The calculated values of K with all methods for mesh I and $N_l = 1$ are listed in Tables 4–6. Some differences from the full 4 × 4-element values are observed. They grow as the We increases, and they are expected to diminish when the mesh is refined (or when N_l is increased). With $N_l = 1$, the maximum relative difference from the 4 × 4-element predictions is less than 0.05%, whereas the total number of unknowns has been reduced by approximately 58%. The computational cost (which is roughly proportional to the number of degrees of freedom times the square of the frontwidth) is reduced by 80%. With the full 2 × 2-element case ($N_l = 0$), the maximum relative difference is bigger than 0.5%, whereas the total number of unknowns and the computational cost are reduced by 64% and 86%, respectively. We should notice that the predictions with the 2 × 2 elements are quite satisfactory at low values of the We. Their main limitation, however, is that they become unstable at moderate values of We.

The advantage of the simultaneous use of 4 × 4 and 2 × 2 stress elements can be better seen with the use of a finer mesh. In Table 7 we summarized the results with Galerkin method for mesh II and different values of N_l. We have observed that the method diverges at low values of We if N_l is small, as does the full 2 × 2-element method. When $N_l = 4$, the maximum difference of the calculated drag correction factors from the full 4 × 4-element values is less then 0.02% whereas the total number of unknowns has been decreased by about 51%. For $N_l = 4$, the thickness of the 4 × 4-element ring is approximately $0.2R$ as is approximately the thickness of the stress boundary layer. (The reader is referred to the paper of Crochet and Legat (1992) who provide graphs of the stresses along the equatorial plane for $We = 0.7$.) The values of K for mesh II and $N_l = 4$ computed with the SUPG and SU methods are compared with the corresponding full 4 × 4-element and full 2 × 2-element values in Tables 8 and 9 respectively. A bigger N_l should be used at higher We for the SUPG method to converge. The SU method converges at higher We when a full 2 × 2-element mesh is used ($N_l = 0$) but the solution is polluted by oscillations for $We > 0.8$.

Table 7. Calculated values of K with the Galerkin method and mesh II. The values in parentheses correspond to unacceptable finite-element solution ($u_{min} < -\varepsilon$)

We	Full 4 × 4	$N_l = 4$	$N_l = 0$
0.0	5.9476	5.9473	5.9473
0.1	5.8622	5.8620	5.8619
0.2	5.6598	5.6596	5.6595
0.3	5.4198	5.4195	5.4193
0.4	5.1873	5.1870	5.1865
0.5	4.9803	4.9801	(4.9808)
0.6	4.8034	4.8032	Diverges
0.7	4.6553	4.6551	
0.8	4.5332	4.5318	
0.9	4.4346	Diverges	
1.0	Diverges		

Table 8. Calculated values of K with the SUPG method and mesh II. The values in parentheses correspond to unacceptable finite-element solution ($u_{min} < -\varepsilon$)

We	Full 4 × 4	$N_l = 4$	$N_l = 0$
0.0	5.9476	5.9473	5.9473
0.1	5.8620	5.8619	5.8618
0.2	5.6598	5.6594	5.6593
0.3	5.4197	5.4193	5.4190
0.4	5.1872	5.1866	5.1862
0.5	4.9801	4.9796	4.9788
0.6	4.8031	4.8026	(4.8013)
0.7	4.6548	4.6544	Diverges
0.8	4.5320	4.5318	
0.9	4.4314	(4.4316)	
1.0	4.3502	Diverges	
1.1	4.2862		
1.2	Diverges		

Table 9. Calculated values of K with the SU method and mesh II. The values in parentheses correspond to unacceptable finite-element solution ($u_{min} < -\varepsilon$)

We	Full 4 × 4	$N_l = 4$	$N_l = 0$
0.0	5.9476	5.9473	5.9473
0.1	5.8565	5.8561	5.8560
0.2	5.6523	5.6519	5.6517
0.3	5.4144	5.4140	5.4138
0.4	5.1873	5.1868	5.1866
0.5	4.9884	4.9880	4.9878
0.6	4.8219	4.8218	4.8216
0.7	4.6864	4.6866	4.6864
0.8	4.5785	4.5791	4.5789
0.9	4.4946	4.4955	(4.4953)
1.0	4.4312	4.4324	(4.4323)
1.1	4.3854	4.3868	(4.3869)
1.2	4.3546	4.3561	(4.3568)
1.3	4.3368	4.3384	(4.3401)
1.4	4.3302	4.3319	(4.3354)
1.5	4.3335	4.3351	(4.3418)
1.6	4.3454	4.3470	(4.3588)
1.7	4.3650	4.3664	(4.3872)
1.8	4.3915	4.3928	(4.4285)
1.9	Diverges	Diverges	(4.4813)
2.0			(4.5421)
2.1			Diverges

The major advantage of the method can be clearly seen in Tables 8 and 9. The 2 × 2 elements show a rather poor performance. At the very moderate cost of including 4 layers of 4 × 4 elements, we are able to extend the range of convergence in terms of the *We*, while the accuracy is very similar to that of the full-4 × 4-element method. We see in Table 8 that, with the SUPG method at $We = 0.8$, we obtain $K = 4.5320$ with full 4 × 4-element coverage and $K = 4.5318$ with $N_l = 4$. The results are even more striking with the SU method. With $N_l = 4$, the method has the same range of convergence in terms of the *We* as the full 4 × 4-element method while the values of K show a relative difference of 3×10^{-4} at $We = 1.8$.

5 Numerical results: $(R_C/R) = 2.5$ and 5

Having gained enough confidence in the simultaneous use of 2 × 2 and 4 × 4 stress elements, we now consider other geometrical ratios, i.e. $(R_C/R) = 2.5$ and 5. The new meshes were constructed to be similar to mesh II in the vicinity of the sphere (Fig. 7). What we will do in the present section is to start the calculations with $N_l = 0$ and then continue with $N_l = 4$. The results for K with the accurate SUPG method are shown in Table 10. It is obvious that the numerical problem is less severe in the present cases compared to the $(R_C/R) = 2$ case.

The calculated drag correction factors with the SUPG method are shown in Fig. 8a. In agreement with Hassager and Bisgaard (1983); Carew and Townsend (1988), K decreases less rapidly with the *We* as the ratio (R_C/R) increases. It is worth noting that as (R_C/R) increases the stress boundary layers weaken and the use of 4 × 4 elements becomes less necessary, for the moderate Weissenberg numbers examined here (see Table 10). The calculated values of K for $(R_C/R) = 5$, for example, are practically the same (up to the first four digits) as those obtained with a full 2 × 2-element mesh. The use of 4 layers of 4 × 4 elements, however, confirms the accuracy of the results.

Figure 8b shows an enlarged view of the graph for $(R_C/R) = 5$. We observe that K reaches a minimum between $We = 1.0$ and 1.1. This minimum appears for $N_l = 0$ as well as for $N_l = 4$.

In Fig. 9, we have plotted the wall correction factors obtained from Table 10 for $We = 0$ and 1 along with Faxen's curve for a Newtonian fluid. For $We = 0$, our results agree with the predictions of Faxen's formula. The wall effect for the viscoelastic fluid is similar to that for the Newtonian fluid for low values of R/R_C, in agreement with experiments (Chmielewski et al. 1990; Tirtaatmadja et al. 1990).

Table 10. Calculated values of K with the SUPG method and different diameter ratios. The values in parentheses correspond to unacceptable finite-element solution ($u_{min} < -\varepsilon$)

We	2:1		2.5:1		5:1	
	$N_l = 4$	$N_l = 0$	$N_l = 4$	$N_l = 0$	$N_l = 4$	$N_l = 0$
0.0	5.9473	5.9473	3.5914	3.5913	1.6795	1.6795
0.1	5.8619	5.8618	5.5697	3.5696	1.6780	1.6780
0.2	5.6594	5.6593	3.5133	3.5133	1.6738	1.6738
0.3	5.4193	5.4190	3.4391	3.4390	1.6677	1.6677
0.4	5.1866	5.1862	3.3606	3.3605	1.6605	1.6605
0.5	4.9796	4.9788	3.2861	3.2860	1.6530	1.6530
0.6	4.8026	(4.8013)	3.2196	3.2195	1.6460	1.6460
0.7	4.6544	Diverges	3.1625	3.1622	1.6400	1.6400
0.8	4.5318		3.1147	3.1143	1.6354	1.6354
0.9	(4.4316)		3.0756	Diverges	1.6323	1.6323
1.0	Diverges		3.0445		1.6309	1.6308
1.1			3.0204		1.6311	1.6310
1.2			3.0026		1.6329	1.6328
1.3			2.9904		1.6362	1.6361
1.4			2.9832		1.6409	1.6408
1.5			2.9808		1.6469	1.6468
1.6			Diverges		1.6541	1.6540

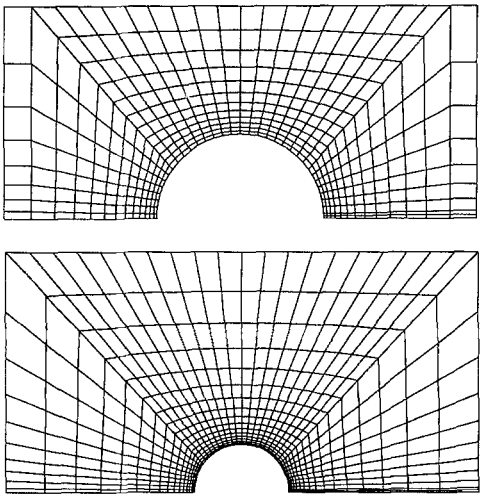

Fig. 7. Central portions of the finite element meshes for $(R_C/R) = 2.5$ and 5

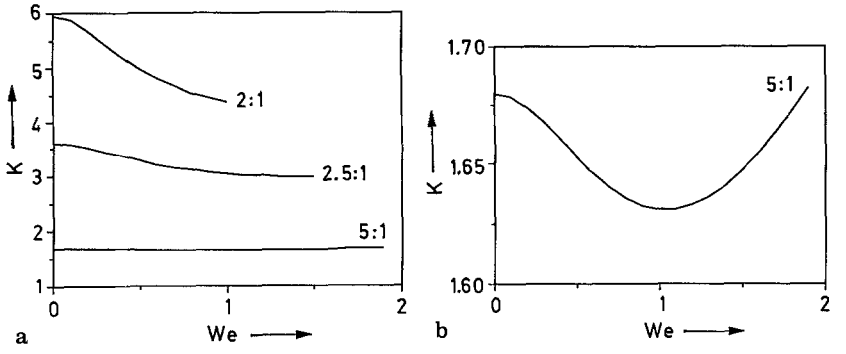

Fig. 8. a Drag correction factors for various values of the ratio R_C/R obtained with the SUPG method and $N_l = 4$; **b** Enlarged view of the graph for $R_C/R = 5$

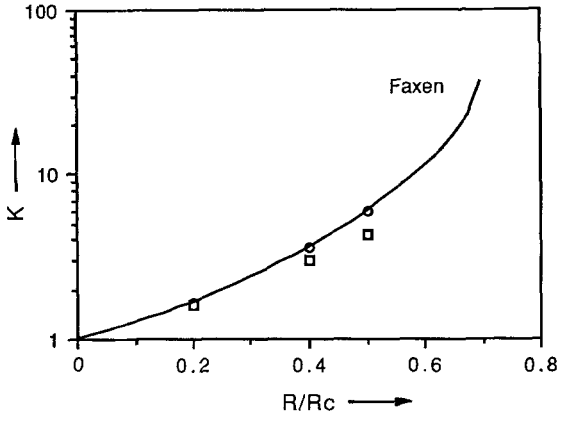

Fig. 9 Calculated wall correction factors compared with the predictions of Faxen's formula; ○: $We = 0$; □: $We = 1$

6 Conclusions

A finite element technique based on the simultaneous use of 4 × 4 and 2 × 2 bilinear stress elements has been proposed for the solution of viscoelastic flow problems. The method has been applied to the creeping motion of a Maxwell fluid past a sphere falling along the axis of a cylindrical tube using the Galerkin, the SUPG and the SU formulations. It has been found that a thin layer of 4 × 4 elements around the surface of the sphere is adequate to assure the accuracy and the stability

of the solution whereas the total number of unknowns is dramatically reduced. The effect of the sphere/cylinder diameter ratio has also been examined.

References

Acharya, A.; Mashelkar, R. A.; Ulbrecht, J.: Flow of inelastic and viscoelastic fluids past a sphere. I Drag coefficient in creeping and boundary-layer flows. Rheol. Acta. 15, 454–470

Babuska, I. (1973): The finite element method with Lagrange multipliers. Numer. Math. 20, 179–192

Brezzi, F. (1974): On the existence, uniqueness and approximation of saddle-point problems arising from Lagrangian multipliers. RAIRO Num. Analysis. 8–R2, 129–151

Brooks, A. N.; Hughes, T. J. R. (1982): Streamline-upwind/Petrov–Galerkin formulations for convection dominated flows with particular emphasis on the incompressible Navier–Stokes equations. Comp. Meth. Appl. Mech. Eng. 32, 199–259

Broadbent, J. M.; Mena, B. (1974): Slow flow of an elasto-viscous fluid past cylinders and spheres. Chem. Eng. J. 8, 11–19

Carew, E. O. A.; Townsend, P. (1988): Non-Newtonian flow past a sphere in a long cylindrical tube. Rheol. Acta. 27, 125–129

Caswell, B.; Schwarz, W. H. (1962): The creeping motion of a non-Newtonian fluid past a sphere. J. Fluid Mech. 13, 417–426

Chhabra, R. P.; Uhlherr, P. H. T.; Boger, D. V. (1980): The influence of fluid elasticity on the drag coefficient of spheres. J. Non-Newtonian Fluid Mech. 6, 187–199

Chhabra, R. P.; Uhlherr, P. H. T. (1988): The influence of fluid elasticity on wall effects for creeping sphere motion in cylindrical tubes. Can. J. Chem. Eng. 66, 154–157

Chilcott, M. D.; Rallison, J. M. (1988): Creeping flow of dilute polymer solutions past cylinders and spheres. J. Non-Newtonian Fluid Mech. 29, 381–432

Chmielewski, C.; Nichols, K. L.; Jayaraman, K. (1990): A comparison of the drag coefficients of spheres translating in corn-syrup-based and polybutene-based Boger fluids. J. Non-Newtonian Fluid Mech. 35, 37–47

Crochet, M. J.; Davies, A. R.; Walters, K. (1984): Numerical simulation of non-Newtonian flow. Elsevier, New York and Amsterdam

Crochet, M. J. (1989): Numerical simulation of viscoelastic flow: a review. In: Rubber Chemistry and Technology, Rubber Reviews. Amer. Chem. Soc. 62, 426–455

Crochet, M. J.; Delvaux, V.; Marchal, J. M. (1990): Numerical simulation of highly viscoelastic flows through an abrupt contraction. J. Non-Newtonian Fluid Mech. 34, 261–268

Crochet, M. J.; Legat, V. (1992): The consistent streamline-upwind/Petrov–Galerkin method for viscoelastic flow revisited. J. Non-Newtonian Fluid Mech. 42, 283–299

Fortin, M.; Pierre, R. (1989): On the convergence of the mixed method of Crochet and Marchal for viscoelastic flows. Comp. Meth. Appl. Mech. Eng. 73, 341–350

Gervang, B.; Davies, A. R.; Phillips, T. N. (1992): On the simulation of viscoelastic flow past a sphere using spectral methods. Int. J. Numer. Methods. Fluids. (to appear)

Giesekus, H. (1963): Rheol. Acta. 3, 59

Harlen, O. G. (1990): High-Deborah-number flow of a dilute polymer solution past a sphere falling along the axis of a cylindrical tube. J. Non-Newtonian Fluid Mech. 37, 157–173

Hassager, O.; Bisgaard, C. (1983): A Lagrangian finite element method for the simulation of flow of non-Newtonian liquids. J. Non-Newtonian Fluid Mech. 12, 153–164

Keunings, R. (1989): Simulation of viscoelastic fluid flow. In: Tucker, III, C.L. (ed): Chapter 9 in Fundamentals of computer modeling for polymer processing. Hanser Publishers, Munich. 403–469

Leslie, F. M. (1961): The slow flow of a visco-elastic liquid past a sphere. Quart. J. Mech. Appl. Math. 14, 36–48

Lunsmann, W.; Brown, R. A.; Armstrong, R. C. (1992): J. Non-Newtonian Fluid Mech. (to appear)

Marchal, J. M.; Crochet, M. J.; Keunings, R. (1984): Adaptive refinement for calculating viscoelastic flows. In: Carey, G. F.; Oden, J. T. (eds): Proceedings of the Fifth International Symposium on Finite Elements and Flow Problems. Austin, Texas, January. 473–478

Marchal, J. M.; Crochet, M. J. (1987): A new mixed finite element for calculating viscoelastic flow. J. Non-Newtonian Fluid Mech. 26, 77–114

Mena, B.; Caswell, B. (1974): Slow flow of an elastic-viscous fluid past an immersed body. Chem. Eng. J. 8, 125–134

Mena, B.; Manero, O.; Leal, L. G. (1987): The influence of rheological properties on the slow flow past spheres. J. Non-Newtonian Fluid Mech. 26, 247–275

Sugeng, F.; Tanner, R. I. (1986): The drag on spheres in viscoelastic fluids with significant wall effects. J. Non-Newtonian Fluid Mech. 20, 281–292

Tiefenbruck, G.; Leal, L. G. (1982): A numerical study of the motion of a viscoelastic fluid past rigid spheres and spherical bubbles. J. Non-Newtonian Fluid Mech. 10, 115–155

Tirtaatmadja, V.; Uhlherr, P. H. T.; Sridhar, T. (1990): Creeping motion of spheres in fluid M1. J. Non-Newtonian Fluid Mech. 35, 327–337

Zheng, R.; Phan-Thien, N.; Tanner, R. I. (1990): On the flow past a sphere in a cylindrical tube: limiting Weissenberg number. J. Non-Newtonian Fluid Mech. 36, 27–49

Zheng, R.; Phan-Thien, N.; Tanner, R. I. (1991): On the flow past a sphere in a cylindrical tube: effects of inertia, shear-thinning and elasticity. Rheol. Acta. 30, 499–510

Communicated by T. E. Tezduyar, August 6, 1992